Adaptive sampling for UAV sensor network in oil spill management

Esten Ingar Grøtli, Joakim Haugen, Tor Arne Johansen and Lars Imsland

***Abstract*— In this paper we propose a method for adaptive sampling using Unmanned Aerial Vehicles (UAVs) in oil spill management. The goal is to measure and estimate oil spill concentrations at the sea surface, while at the same time identify the leak rates of sources at known positions. First we construct a cost which approximates the benefit of sampling locations at specific times. This cost is based on measures of observability and of persistency of excitation for the oil spill model. A receding horizon Mixed-Integer Linear Programming (MILP) problem is solved in order to find UAV trajectories which are optimal with respect to the cost. For UAV trajectory tracking we use a Lyapunov based controller. The oil spill concentration measurements taken by the UAVs by following these tracks are used in an adaptive observer, which provides state (concentration) and parameter (leak rate) estimates. Under the assumption that the sampling strategy described above lead to uniform complete observability and persistency of excitation, we prove Uniform Global Asymptotic Stability (UGAS) of the state estimation, parameter identification and UAV trajectory tracking errors. Finally, we provide a simulation of the proposed strategy, and compare it with two other strategies.**

I. Introduction

In this paper the goal is to measure and estimate the states of a Distributed Parameter System (DPS) using UAVs equipped with the appropriate sensors and communication units. We will employ a strategy called *adaptive sampling* where the times and locations for taking new measurements are proposed based on a model of the process and previous measurements. For illustration purpose we apply our findings in an application within *oil-spill management*. Oil-spill management can be defined as the process of detecting, tracking and cleaning up after an oil-spill. We will here solve the specific task of estimating the oil spill concentration on the sea surface, and at the same time identify the leak rates of two moving ships at known positions.

Numerous works have considered the problem of finding trajectories of sensor nodes in order to estimate states and identify parameters of DPSs in an optimal manner, e.g. [1], [2], [3], [4], [5], [6], [7].

The main contribution of this paper is the proposal of a new sampling strategy, for which we can provide strong stability guarantees of the state estimation, parameter identification and trajectory tracking errors. A Mixed Integer Linear Programming (MILP) problem is solved in order to find trajectories for the UAVs which maximize measures of observability and persistency of excitation, while at the same time satisfy collision avoidance and anti-winding constraints. In particular, the formulation of the objective is new compared to [8]. The state estimator and UAV controller, although similar to [4], [6], have some characteristic and new properties:

- We consider the *joint* state estimation and parameter identification problem, where as only the state estimation problem was considered by [4].
- In [4] and [6] the closed-loop and open-loop linear DPS state matrices, respectively, are assumed to be exponentially stable. In this paper this assumption is replaced by the weaker requirement that the state- and output matrix pair is uniform completely observable. We argue that this is a reasonable assumption, as our sampling strategy is aimed at satisfying this requirement.
- Under our assumptions we are able to prove UGAS of the equilibrium point of the combined state- and parameter error dynamics and UAV tracking error dynamics. In [4] only stability was proved (although their Lyapunov analysis also included collision avoidance and network constraints, which is handled by the trajectory planner in this paper).

II. Modeling

A. Continuum Model

We consider an open, connected spatial domain Ω of interest, where we want to measure and estimate the DPS state. Let the distributed parameter be given by $c(p,t)$, which represent the concentration of oil at the sea surface at some time t, and at a position $p = [\chi, y]^\top \in \mathbb{R}^2$ in east- and north directions, respectively. The concentration is assumed to follow the advection-diffusion Partial Differential Equation (PDE):

$$\frac{\partial c(p,t)}{\partial t} + \nabla(a(p,t)c(p,t)) = \nabla(d\nabla c(p,t)) + f(p,\theta,t)\,, \tag{1}$$

with boundary and initial conditions

$$\frac{\partial c(p,t)}{\partial \mu} = \kappa(p)\,, \quad \text{for } p \in \Sigma_1 \subseteq \partial\Omega \tag{2}$$

$$c(p,t) = \rho(p)\,, \quad \text{for } p \in \Sigma_2 \subseteq \partial\Omega \tag{3}$$

$$c(p,0) = c_0(p)\,, \quad \text{for } p \in \Omega\,. \tag{4}$$

where $a(p,t)$ is the velocity field causing advection, d is the diffusion constant, $f(p,\theta,t)$ represents source terms, $\partial\Omega$ is the boundary of $\Omega \subset \mathbb{R}^2$, and $\Sigma_1, \Sigma_2 \subseteq \partial\Omega$ such that $\Sigma_1 \cup \Sigma_2 = \partial\Omega$. The set Σ_1 contains the Neumann boundary conditions, where as Σ_2 contains the Dirichlet boundary conditions. Out of simplicity we will assume that only the

E. I. Grøtli is with Department of Mathematics and Cybernetics, SINTEF Digital; J. Haugen is with Department of Energy and Transport, SINTEF Ocean; T. A. Johansen and L. Imsland are with Department of Engineering Cybernetics, Norwegian University of Science and Technology. Contact: EstenIngar.Grotli@sintef.no

This is the author accepted version of an article published in
2021 American Control Conference (ACC)
https://doi.org/10.23919/ACC50511.2021.9482819

source terms f are dependent on the vector of unknown parameters, $\theta \in \mathbb{R}^{N_\theta}$. We spatially discretize the advection-diffusion equation using a second-order central discretization scheme, where we for simplicity assume a rectangular area of interest, such that $\bar{\Omega} := \Omega \cup \partial\Omega = [0, L_x] \times [0, L_y]$, with spatial discretization step size d_{xy}. The average value of c in the grid cells can then be approximated by the following Ordinary Differential Equation (ODE):

$$\dot{c} = A(t)c + B(t)\theta\,, \tag{5}$$

where $A \in \mathbb{R}^{N_x N_y \times N_x N_y}$ is a (known) state matrix representing advection- and diffusion effects, $B \in \mathbb{R}^{N_x N_y \times N_\theta}$ is a (known) input matrix representing the effects from the source terms. N_x and N_y are the number of interior grid cells in the east- and north directions, respectively, such that $L_x = d_{xy} N_x$ and $L_y = d_{xy} N_y$. The value of $c(p,t)$ at some location $p = p_{m,n} = [d_{xy}m, d_{xy}n]^\top$, with $(m,n) \in \mathcal{I}_1^{N_x} \times \mathcal{I}_1^{N_y}$, and where

$$\mathcal{I}_a^b := \{a, a+1, \ldots, b\}, \quad a, b \in \mathbb{Z}\,, \tag{6}$$

is given by $c_{m,n}$, and are arranged in the state vector $c \in \mathbb{R}^{N_x N_y}$ in an east-to-west then south-to-north ordering, also called *natural ordering* [9, page 631].

B. Measurement Matrix Model

By primarily relying on measurements from UAVs equipped with the appropriate sensors, the output equation can be written

$$y = C(q(t))c\,, \tag{7}$$

where $C(q(t)) := \operatorname{col}[C_1(q_1(t)), \ldots, C_N(q_N(t))]$ with C_i being the output matrix of sensor i, $q := \operatorname{col}[q_1, \ldots, q_N]$, and $q_i = [x_i, y_i]^\top \in \mathbb{R}^2$ being the time-varying position of UAV number i in the east- and north directions, and N being the total number of UAVs. The realization of the measurement operator $C(q(t))$ used in this paper is taken from [6]. Since the model is spatially discretized we use weighting surfaces to describe how the sensors measure the discretized process variables. We assume that the grid points of the discretized process are coarsely distributed, at least compared to the field-of-view of the sensor on board the UAV, which means that at most the four closest discretization points will influence the measurement operator. Mathematically, this means that for any given position $q_i \in \Omega$, and for any discretization point $(m,n) \in \mathcal{I}_1^{N_x} \times \mathcal{I}_1^{N_y}$,

$$w_{m,n}(q_i) > 0 \iff \left|q_i - q_{m,n}\right|_\infty < d_{xy}\,, \tag{8}$$

where $w_{m,n}$ is a weighting surface, $q_{m,n} = [d_{xy}m, d_{xy}n]^\top$. Then, by assuming that the position of the UAV q_i is contained in a box of the grid cells $(p_{v,w}, p_{v+1,w}, p_{v+1,w+1}, p_{v,w+1})$, the measurement matrix $C_i(q_i) \in \mathbb{R}^{4 \times N_x N_y}$, can be written as [6]

$$\begin{aligned} &C_i(q_i) = \\ &[w_{v,w}(q_i)]_{1,(w-1)N_x+v} + [w_{v+1,w}(q_i)]_{2,(w-1)N_x+v+1} + \\ &[w_{v,w+1}(q_i)]_{3,wN_x+v} + [w_{v+1,w+1}(q_i)]_{4,wN_x+v+1}\,, \end{aligned} \tag{9}$$

where the weighting functions are indexed in correspondence with the order of the state vector (natural ordering), and where $[a]_{i,j}$ is an all-zero matrix with appropriate dimensions, except at index (i,j) where the element is a.

C. Input Matrix Model Moving Sources

We consider the oil spill being caused by a number of moving sources, and that we try to identify the leak rate of each of them. The number of moving sources is therefore equal to the number of unknown parameters, N_θ. The position of the sources are given by $\xi(t) := \operatorname{col}[\xi_1(t), \ldots, \xi_{N_\theta}(t)]$, with $\xi_i(t) \in \mathbb{R}^2$ being the time-varying position of source number i in the east- and north directions. In a similar way as we use weighting functions to describe how the sensors measure the discretized process variables in the measurement model, we will employ a weighting function to describe how the motion of the sources influences the process variables. Let $B(\xi) := [B_1(\xi_1), \ldots, B_{N_\theta}(\xi_{N_\theta})]$. If the position of the leaking source ξ_i is contained in $(p_{v,w}, p_{v+1,w}, p_{v+1,w+1}, p_{v,w+1})$ the matrix $B_i(\xi_i) \in \mathbb{R}^{N_x N_y}$, can be written as

$$\begin{aligned} &B_i(\xi_i) = \\ &[w_{v,w}(\xi_i)]_{(w-1)N_x+v,1} + [w_{v+1,w}(\xi_i)]_{(w-1)N_x+v+1,1} + \\ &[w_{v,w+1}(\xi_i)]_{wN_x+v,1} + [w_{v+1,w+1}(\xi_i)]_{wN_x+v+1,1}\,, \end{aligned} \tag{10}$$

where the weighting functions and the matrix $[\cdot]$ were introduced in the previous section.

D. UAV Model

We assume that the UAVs are fully actuated (holonomic), and the model for the UAVs motion is given by

$$\dot{q}_i = r_i \tag{11}$$

$$\dot{r}_i = M_i^{-1}(-D_i r_i + f_i)\,, \tag{12}$$

for any $i \in \mathcal{I}_1^N$, where $q_i, r_i, f_i \in \mathbb{R}^2$ are the position-, velocity and control force vectors of vehicle i, respectively, in the east- and north directions, and where $M_i, D_i \in \mathbb{R}^{2\times 2}$ are matrices of constant parameters for mass-, and damping effects, respectively.

III. Estimation and motion planning

We will now give an overview of the proposed estimation, identification and trajectory planning strategy. The purpose behind each part of the strategy is motivated with the oil spill example introduced in Section I, and illustrated in Figure 1.

State- and parameter estimator: This is a centralized estimator located at the ground control station. In the oil spill example the state matrix $A(t)$ depends on the weather- and ocean data, the input matrix $B(t)$ depends on the motion of the source ships which is assumed available through broadcast (e.g. using the Automatic Identification System (AIS) which is required used internationally for most ships over a certain size), and the output matrix $C(q(t))$ depends on the positions q of the UAVs. In this paper an adaptive observer is used to estimate the state vector and identify

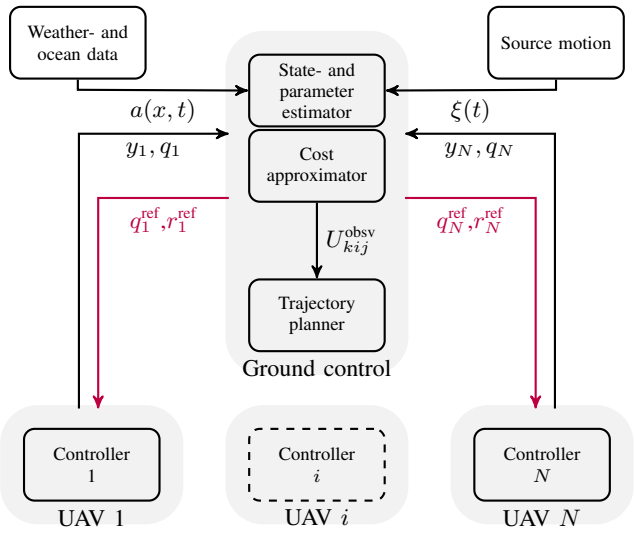

Fig. 1. Motion planning strategy: The source motion $\xi(t)$, weather- and ocean data $a(x,t)$ and measurement from the UAVs $y(q(t))$ are used in the centralized state- and parameter estimator. Based on $\xi(t)$ and $a(p,t)$, the a cost U_{kmn}^{obsv} is created emphasizing where and when to make measurements, based on observability and persistency of excitation measures. This cost matrix is used by the trajectory planner, to find the trajectories which over the predicted horizon are optimal. Trajectory $q_i^{\text{ref}}, r_i^{\text{ref}}$ is transmitted to UAV i and used as a reference for a Lyapunov based tracking controller.

unknown parameters.

Cost approximator: The knowledge of the current state, the state matrix $A(t)$ and the input matrix $B(t)$ is used to approximate the cost of sampling the distributed process a specific location at a specific time. In this paper, we calculate an observability measure based on the least singular value of the observability matrix of the extended system, that is, a system where the state vector is extended to also include the unknown parameters. Improving the observability measure by taking measurements at the best locations and times would consequently lead to reduced state estimation and parameter identification errors.

Trajectory planner: The approximated cost function is then used in a MILP planning problem over a finite horizon. The optimization problem includes collision avoidance constraints and anti-winding constraints. As the output of the planning problem is an ordered set of discrete positions for each of the UAVs, interpolation is used to create smooth reference signals for the tracking controller.

Tracking controller: Finally a tracking controller based on Lyapunov theory is implemented to make the UAVs track the references created by the trajectory planner.

A. Tracking controller

Let $q_i^{\text{ref}}(t)$, $r_i^{\text{ref}}(t)$ $\dot{r}_i^{\text{ref}}(t)$ be sufficiently smooth reference signals generated by the trajectory planner. Then, by defining $\tilde{q}_i(t) := q_i(t) - q_i^{\text{ref}}(t)$ and $\tilde{r}_i(t) := r_i(t) - r_i^{\text{ref}}(t)$, as the position- and velocity errors, the error dynamics with respect to the reference motion is given by

$$\dot{\tilde{q}} = \tilde{r} \tag{13}$$

$$\dot{\tilde{r}} = -\dot{r}^{\text{ref}} + M^{-1}(-D(\tilde{r} + r^{\text{ref}}) + f)\,, \tag{14}$$

where $\tilde{q} = \text{col}[\tilde{q}_1, \ldots, \tilde{q}_N]$, $\tilde{r} = \text{col}[\tilde{r}_1, \ldots, \tilde{r}_N]$, $q^{\text{ref}} = \text{col}[q_1^{\text{ref}}, \ldots, q_N^{\text{ref}}]$, $r^{\text{ref}} = \text{col}[r_1^{\text{ref}}, \ldots, r_N^{\text{ref}}]$, $M := \text{blkdiag}[M_1, \ldots, M_N]$, $D := \text{blkdiag}[D_1, \ldots, D_N]$, and where we have assumed that $r_i^{\text{ref}} = \dot{q}_i^{\text{ref}}$ for any $i \in \mathcal{I}_1^N$.

Our feedback controller, similar to the controller derived by vectorial backstepping for a mass-damper-spring system in [10, Page 277], is given by:

$$f(t) = M\dot{r}^{\text{vir}} + Dr^{\text{vir}} - K^{\text{pro}}\tilde{q} - K^{\text{der}}(\tilde{r} + \Lambda\tilde{q})\,, \tag{15}$$

with $r^{\text{vir}} := r^{\text{ref}} - \Lambda\tilde{q}$ being a virtual reference signal, $\Lambda := \text{blkdiag}[\Lambda_1, \ldots, \Lambda_N]$ with $\Lambda_i \in \mathbb{R}^{2\times 2}$ a positive definite diagonal matrix for any $i \in \mathcal{I}_1^N$, $K^{\text{pro}} := \text{blkdiag}[K_1^{\text{pro}}, \ldots, K_N^{\text{pro}}]$ with $K_i^{\text{pro}} \in \mathbb{R}^{2\times 2}$ a symmetric positive definite matrix for any $i \in \mathcal{I}_1^N$, and $K^{\text{der}} := [K_1^{\text{der}}, \ldots, K_N^{\text{der}}]$ with $K_i^{\text{der}} \in \mathbb{R}^{2\times 2}$ a positive definite matrix for any $i \in \mathcal{I}_1^N$. The motivation behind requiring Λ, K^{der}, K^{pro} as diagonal or block diagonal matrices, is to maintain a decentralized implementation, where the motion of one vehicle is independent of the motion of the others, except through the reference trajectory. For future reference, we notice that the closed-loop error dynamics can now be written as

$$\dot{\tilde{q}} = \tilde{r} \tag{16}$$

$$\dot{\tilde{r}} = -\Lambda\tilde{r} + M^{-1}(-(D + K^{\text{der}})(\tilde{r} + \Lambda\tilde{q}) - K^{\text{pro}}\tilde{q})\,. \tag{17}$$

B. State- and parameter estimator

Here, we apply the adaptive observer of [11]. The main motivation for using this observer is that uniform asymptotic stability of the state- and parameter estimation errors are guaranteed with relaxed assumptions compared to the Kalman filter, see [11] for details. First, through output injection, equations (5) and (7), are transformed to

$$\dot{c} = A^{\text{cl}}(t,q)c + B(t)\theta + L(t)y\,, \tag{18}$$

$$y = C(q)c\,, \tag{19}$$

where $A^{\text{cl}}(t,q) = A(t) - L(t)C(q)$, and $L(t)$ is a time varying matrix to be designed. Again we emphasize that θ is an unknown *constant* parameter. By defining the dynamic transformation $z(t) = c(t) - \Psi(t)\theta$, where $\Psi(t) \in \mathbb{R}^{N_x N_y}$ is the solution to the equation

$$\dot{\Psi} = A^{\text{cl}}(t,q)\Psi + B(t)\,, \tag{20}$$

with some user specified, finite initial condition $\Psi(0) = \Psi_0$, the transformed system can be written

$$\dot{z} = A^{\text{cl}}(t,q)z + L(t)y\,, \tag{21}$$

$$y = C(q)[z + \Psi(t)\theta]\,. \tag{22}$$

The adaptive observer proposed in [11], [12] for this system is

$$\dot{\hat{z}} = A^{\text{cl}}(t,q)\hat{z} + L(t)y\,, \tag{23}$$

$$\dot{\hat{\theta}} = \gamma\Psi^{\top}(t)C^{\top}(q)[y - C(q)\hat{z} - C(q)\Psi(t)\hat{\theta}]\,, \tag{24}$$

where $\hat{\theta}$ is the estimate of the unknown parameter θ, and $\gamma \in \mathbb{R}^{N_\theta \times N_\theta}$ is a user specified positive definite, diagonal matrix.

C. Closed-loop system

To analyse the convergence and stability properties of the system we will now calculate the closed-loop dynamics. To that end define $\chi := \text{col}[\chi_1, \chi_2, \chi_3]$, where $\chi_1 = \text{col}\,[\chi_{11}, \chi_{12}] = \text{col}\,[\tilde{q}, \tilde{r}]$ is the tracking error of the controller, $\chi_2(t) = \theta - \hat{\theta}(t)$ is the parameter identification error and $\chi_3(t) = z(t) - \hat{z}$ is the state estimation error. These error variables are the solutions to

$$\dot{\chi}_1 = A_1\chi_1 \tag{25}$$

$$\dot{\chi}_2 = f_2(t, \chi_{11})\chi_2 + g_2(t, \chi_{11})\chi_3 \tag{26}$$

$$\dot{\chi}_3 = A_3(t, \chi_{11})\chi_3 \tag{27}$$

where A_1 is given by (28),

$$f_2(t, \chi_{11}) := -\gamma\Psi^\top(t)C^\top(t, \chi_{11})C(t, \chi_{11})\Psi(t)\,, \tag{29}$$

$$g_2(t, \chi_{11}) := -\gamma\Psi^\top(t)C^\top(t, \chi_{11})C(t, \chi_{11})\,, \tag{30}$$

and finally $A_3(t, \chi_{11}) := A^{\text{cl}}(t, \chi_{11} + q^{\text{ref}}(t))$. With a slight abuse of notation, we have redefined the measurement matrix to emphasize that it depends on both the state and reference trajectory, that is $C(t, \chi_{11}) := C(\chi_{11} + q^{\text{ref}}(t)) = C(q)$. We see that by moving the dependence on the unknown parameter from the state equation in (18)-(19) to the output equation in (21)-(22), the dynamics of the state estimation errors (27) becomes independent of the convergence of the parameter identification error. We see that the stability properties of (27) depends on the motion of the UAVs through $C(t, \chi_{11})$ and $L(t)$, since $A_3(t, \chi_{11}) = A(t) - L(t)C(t, \chi_{11})$. The second term on the right hand side of (26) vanishes with the state estimation error χ_3. If this term is ignored, (26) is exponentially stable if the persistency of excitation condition is satisfied [11].

D. Main result

Before we present the main result, we will present some needed assumptions.

Assumption 1: There exist a positive constant c_0 such that $|q^{\text{ref}}(t)| < c_0$ and $|r^{\text{ref}}(t)| < c_0$ for any $t \geq 0$.

Assumption 2: The matrices $A(t)$ and $B(t)$ of (5) are known, and there exist positive constants c_1 and c_2 such that $\left|A(t)\right| \leq c_1$ and $\left|B(t)\right| \leq c_2$ for any $t \geq 0$.

Assumption 3: The measurement matrix $C(t, \chi_{11})$ (recall $C(t, \chi_{11}) := C(\chi_{11} + q^{\text{ref}}(t)) = C(q)$ with $C(q)$ of (7)) is known, and for bounded arguments χ_{11} and $q^{\text{ref}}(t)$ there exists a constant c_3 such that $\left|C(t, \chi_{11})\right| \leq c_3$ for any $t \geq 0$.
Assumptions 1-3 are reasonable from a practical viewpoint and simplifies our analysis.

Assumption 4 (Assumption on observability): The pair $(A(t), C(t, \chi(t)))$ is uniformly completely observable, *cf.* [13].

Assumption 5 (Assumption on persistency of excitation): There exist positive constants t_0, T and μ such that $G(t_0, t+T) \geq \mu I$ holds for any $t \geq t_0$, where

$$G(t_0, t+T) = \int_{t_0}^{t+T} \Psi^\top(\tau)C^\top(\tau, \chi_{11}(\tau))C(\tau, \chi_{11}(\tau))\Psi(\tau)\,\mathrm{d}\tau\,. \tag{31}$$

Remark 1: Notice that in Assumption 5 the assumption is on persistency of excitation of $\Psi(\cdot)$. However, since Ψ is dependent on $B(\cdot)$ through (20) it is in essence also a persistency condition on B. This means that the motion of the leaking ships can influence the persistency of excitation condition.
Assumption 4 and 5 are highly dependent of the positions of the UAVs, q through the measurement matrix $C(t, \chi_{11})$, where $\chi_{11} = \tilde{q} = q - q^{\text{ref}}$. The objective of the trajectory planner of Section III-F is therefore to find reference trajectories $q^{\text{ref}}(t)$ such that the assumptions are satisfied.

From the dual to [14, Lemma 1] we have that due to Assumption 2, Assumption 4 is equivalent to the existence of a constant δ such that the observability Gramian W defined as

$$W(t, t+\delta) = \int_{t}^{t+\delta} \Phi^\top(\tau, t)C^\top(\tau, \chi_{11}(\tau))C(\tau, \chi_{11}(\tau))\Phi(\tau, t)\,\mathrm{d}\tau \tag{32}$$

satisfies $0 \leq c_6(\delta) \leq W(t, t+\delta) \leq c_7(\delta)$ for some constants c_6, c_7, and $\Phi(\cdot, \cdot)$ is the state transition matrix associated with (5). This means that it is possible to render the state estimation error dynamics (27) Uniformly Exponentially Stable (UES) by an appropriate choice of the observer gain matrix $L(t)$ introduced in (18). For instance, it can be chosen by Kalman filter design as in [15], [16, Theorem 1], [17]:

$$L(t) = P_3(t)C^\top(t, \chi_{11}(t))R_3^{-1}(t) \tag{33}$$

where $P_3(t)$ is the solution to the forward differential Riccati equation,

$$\begin{aligned}\dot{P}_3 =& A(t)P_3(t) + P_3(t)A^\top(t) + Q_3(t) \\ &- P_3(t)C^\top(t, \chi_{11}(t))R_3^{-1}(t)C(t, \chi_{11}(t))P_3(t)\end{aligned} \tag{34}$$

with $P_3(0)$ positive definite and symmetric, and where $Q_3(t)$, $R_3(t)$ satisfies the following assumption:

Assumption 6: The user specified matrices $Q_3(t)$, $R_3(t)$ are both positive definite and uniformly bounded, that is, there exist constants c_8 and c_9 such that $\left|Q_3(t)\right| \leq c_8$ and $\left|R_3(t)\right| \leq c_9$ are satisfied for any $t \geq 0$.
This choice for $L(t)$ was used in [18], where the objective is similar to that of this paper.

We are now ready to state the main result:

Theorem 1: Under Assumptions 1-6 the equilibrium point $\chi = 0$ of (25)-(27) is UGAS.
The proof of the theorem is given in the Appendix.

E. Cost approximator

The purpose of the cost approximator is to construct the matrix U^{obsv}_{kmn}, which elements are correlated to the benefit of taking measurements at some grid point (m, n) in the

$$A_1 := \begin{bmatrix} 0 & 1 \\ -M^{-1}((D+K^{\text{der}})\Lambda + K^{\text{pro}}) & -\Lambda - M^{-1}(D+K^{\text{der}}) \end{bmatrix} \tag{28}$$

discretized area, at k time steps into the future. The construction of U^{obsv}_{kmn}, is based on the observability Gramian of the *extended system*. In fact, to take the motions of the sources into account when calculating the observability measure, we rewrite the state equations, (5)-(7), as:

$$\dot{\tilde{c}} = \tilde{A}(t)\tilde{c}\,, \tag{35}$$
$$y = \tilde{C}(q(t))\tilde{c}\,, \tag{36}$$

with

$$\tilde{A}(t) = \begin{bmatrix} A(t) & B(t) \\ 0 & 0 \end{bmatrix}, \tag{37}$$

$$\tilde{c} = \begin{bmatrix} c \\ \theta \end{bmatrix}, \quad \tilde{C}(q(t)) = \begin{bmatrix} C(q(t)) & 0 \end{bmatrix}, \tag{38}$$

where an interesting property of this extended system is given in the next theorem:

Theorem 2: Let Assumption 2 hold. Then uniform complete observability of the pair $(\tilde{A}(t), \tilde{C}(q(t)))$, implies Assumption 4 and Assumption 5, that is uniform complete observability of (5)-(7) *and* persistency of excitation on $\Psi(t)$.

Proof: By Assumption 2, the matrices $\tilde{A}(t)$ and $\tilde{C}(q(t))$ are uniformly bounded. Uniform complete observability of the pair $(\tilde{A}(t), \tilde{C}(q(t)))$ implies that the observability Gramian of the extended system (35)-(36) is positive definite and bounded. In [12, Appendix] it is shown that the observability Gramian associated with the pair $(\tilde{A}(t), \tilde{C}(q(t)))$ of the extended system, has G of (31) *and* W of (32) along its diagonal. The conclusion follows. ∎

To get information about where measurements should be taken, we will in the following explain the construction of the three-dimensional matrix U^{obsv}_{kmn} which approximates how beneficial it is to make measurements in a certain area (m, n) at some time step k. First, consider $\bar{\Omega}$ divided into equally large non-overlapping areas, such that the areas make up the whole of $\bar{\Omega}$, and predict the effect on the observability Gramian of the extended system by static measures in each of these areas for some prediction horizon. The areas can consist of multiple grid cells, such that $D_{\chi y} = \gamma_{\chi y} d_{\chi y}$, where $\gamma_{\chi y} \in \mathbb{Z}$ and $D_{\chi y}$ is the length of the sides of the square areas. The prediction is based on actual measurements for a horizon $T_{\underline{H}}$ into the past *and* assumed static measurements taken at area (m, n) for a horizon $T_{\overline{H}}$ into the future. The observability Gramian associated with the extended system is given by

$$\begin{aligned} &\tilde{W}^t_{m,n}(T_{\underline{H}}, T_{\overline{H}}) = \\ &\int_{T_{\underline{H}}}^{t} \tilde{\Phi}^\top(\tau, T_{\underline{H}})\tilde{C}^\top(q(\tau))\tilde{C}(q(\tau))\tilde{\Phi}(\tau, T_{\underline{H}})\,\mathrm{d}\tau \\ &+ \int_{t}^{T_{\overline{H}}} \tilde{\Phi}^\top(\tau, t)\tilde{C}^\top(Q_{m,n})\tilde{C}(Q_{m,n})\tilde{\Phi}(\tau, t)\,\mathrm{d}\tau\,, \end{aligned} \tag{39}$$

where $\tilde{\Phi}(\cdot,\cdot)$ is the state transition matrix associated with (35) and $Q_{m,n} = [D_{\chi y} m, D_{\chi y} n]$. At each time step $k = t/D_t \in \mathcal{I}_1^{N_{\overline{H}}}$, where D_t is the sample interval of the motion planner and $N_{\overline{H}} = T_{\overline{H}}/D_t - 1$, and for any, $m \in \mathcal{I}_1^{N_x/\gamma_x}$, $n \in \mathcal{I}_1^{N_y/\gamma_y}$ take

$$U^{\text{obsv}}_{kmn} = 1/\sigma_{\min}(\tilde{W}^k_{m,n})\,. \tag{40}$$

Here, $\sigma_{\min}(\cdot)$ is the minimum singular value. For simplicity of implementation we integrate forward in time the system of differential equations

$$\begin{aligned} \frac{\mathrm{d}}{\mathrm{d}s}\tilde{W}^t_{m,n}(T_{\underline{H}}, s) =& \tilde{\Phi}^\top(s, T_{\underline{H}})\tilde{C}^\top(s)\tilde{C}(s)\tilde{\Phi}(s, T_{\underline{H}})\,, \\ \frac{\mathrm{d}}{\mathrm{d}s}\tilde{\Phi}(s, T_{\underline{H}}) =& \tilde{A}(s)\tilde{\Phi}(s, T_{\underline{H}}) \end{aligned} \tag{41}$$

where $\tilde{\Phi}(T_{\underline{H}}, T_{\underline{H}})$ being the identity matrix is used as initial condition, similar to what is done in [19, Page 21].

F. Trajectory planner

The planning problem follows closely the approach of [8], and the interested reader is referred thereto for more details. The objective function to be minimized is given by

$$J^{\text{obsv}} = \sum_{i=1}^{N}\sum_{k=1}^{N_{\overline{H}}}\sum_{m=1}^{N_x}\sum_{n=1}^{N_y} U^{\text{obsv}}_{kmn}\Gamma_{ikmn}\,, \tag{42}$$

which quantify the benefit at being at a specific position at a specific time. Here, U^{obsv}_{kmn} is given by (40) which contain the unobservability index of area (m, n) at some time step k, while $\Gamma_{ikmn} = 1$ if UAV i is in area (m, n) at time step k, and $\Gamma_{ikmn} = 0$ otherwise. The solution to the optimization problem is an ordered set of positions (centres of the considered areas) for each of the UAVs, and interpolation is therefore used to create smooth reference trajectories.

IV. Simulations

We will in this section consider joint estimation of concentration in an offshore oil spill and identification of the constant leak rates from two sources. The region we consider is $\bar{\Omega} = [0, 500] \times [0, 500]$. The UAV model and controller parameters are found in Table I, the cost approximator and trajectory planner parameters in Table II and finally the observer parameters in Table III. Cubic spline interpolation is used to find the reference trajectories q^{ref}, r^{ref} and $\dot{r}^{\text{ref}}$ from the positions found by solving the MILP problem in the trajectory planner. In the implementation of the measurement model we follow [6]: We define $w_{m,n}(q_{m,n}) = 1$ and

TABLE I

UAV MODEL AND TRACKING CONTROLLER PARAMETERS

Parameter	Value	Parameter	Value
$q_1(0)$	$(25, 25)^\top$ m	$r_1(0)$	$(13, 13)^\top$ m s^{-1}
$q_2(0)$	$(100, 100)^\top$ m	$r_2(0)$	$(15, 15)^\top$ m s^{-1}
D_i	1 kg s^{-1}	M_i	30 kg
K_i^{pro}	diag (1.3159, 1.3159)	K_i^{der}	diag (6.2835, 6.2835)
Λ_i	diag (0.001, 0.001)		
N	2		

TABLE II

COST APPROXIMATOR AND TRAJECTORY PLANNER PARAMETERS

Parameter	Value	Parameter	Value
D_{xy}	50 m	γ_{xy}	1

$w_{m,n}(q_{m\pm1,n\pm1}) = 0$, and we get that

$$w_{m,n}(p) = \begin{cases} \frac{(x-x_{m-1})(y-y_{n-1})}{(x_m-x_{m-1})(y_n-y_{n-1})}, (x,y) \in [x_{m-1}, x_m] \times [y_{n-1}, y_n] \\ \frac{(x-x_m)(y_n-y)}{(x_{m+1}-x_m)(y_n-y_{n-1})}, (x,y) \in [x_m, x_{m+1}] \times [y_{n-1}, y_n] \\ \frac{(x_m-x)(y-y_n)}{(x_m-x_{m-1})(y_{n+1}-y_n)}, (x,y) \in [x_{m-1}, x_m] \times [y_n, y_{n+1}] \\ \frac{(x_{m+1}-x)(y_{n+1}-y)}{(x_{m+1}-x_m)(y_{n+1}-y_n)}, (x,y) \in [x_m, x_{m+1}] \times [y_n, y_{n+1}] \\ 0 \quad , \quad \text{otherwise.} \end{cases} \tag{43}$$

The oil spill parameters of the simulation is given in Table IV. We use a similar flux field as in [2], which is given by

$$a(t,p) = \frac{12}{3600}\left(y - x - \frac{t}{6}, \frac{t(2x-1000)}{600} + y - 1000\right)^\top. \tag{44}$$

We consider only Dirichlet boundary conditions in this example, so $\Sigma_1 = \varnothing$ and $\Sigma_2 = \partial\Omega$. For illustration purpose we will assume two leaking sources. The motion of the first source term is given by

$$\begin{aligned} \xi_1(t) =& 500\left(\frac{\sqrt{5}}{4}\sin\left(\frac{\omega_1 t}{600} + \omega_0\right),\right. \\ & \left. 0.5 + \frac{\sqrt{5}}{4}\cos\left(\frac{\omega_1 t}{600} + \omega_0\right)\right)^\top, \end{aligned} \tag{45}$$

with $\omega_1 = 2\arcsin(0.2\sqrt{5})$ and $\omega_0 = \arcsin(0.4\sqrt{5})$, where as the motion of the second is given by $\xi_2(t) = \frac{1}{2}\xi_1(t)$. The DPS system is simulated for 30 seconds before the estimation based on measurements from the UAVs is started. For the parameter update law (24), we use $\gamma = I$.

TABLE III

OBSERVER PARAMETERS

Parameter	Value	Parameter	Value
$P_3(0)$	$100I$	$\Psi(0)$	0
$R(t) = R$	I	$Q(t) = Q$	I

TABLE IV

OIL SPILL PARAMETERS

Parameter	Value	Parameter	Value
L_x, L_y	500 m	$c(0)$	0 g m^{-2}
d_{xy}	50 m	$\theta(t)\,, \forall t \in [-50, 300]$	0.05 g s^{-1}
N_x, N_y	9		
d	60×10^{-6} m^2 s^{-1}		

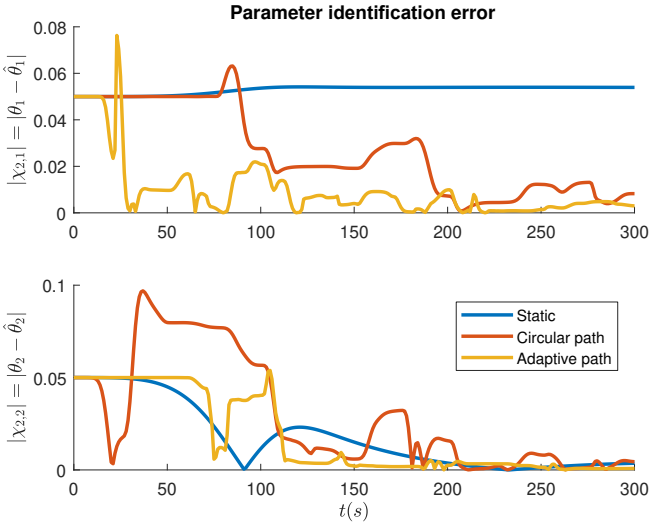

Fig. 2. Oil management: Parameter identification errors with different types of planning strategies. θ_1 and θ_2 are the leak rates from the two sources.

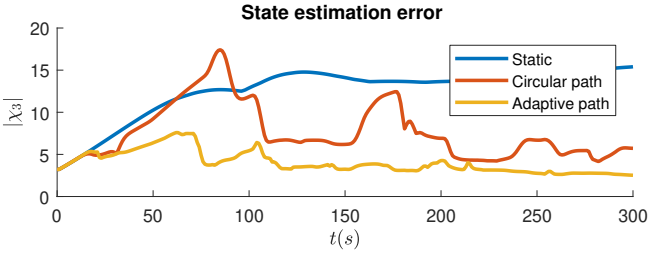

Fig. 3. Oil management: State estimation errors with different types of planning strategies. χ_3 is the estimation error for the sea surface oil concentration.

The parameter identification and state estimation errors are illustrated in Figure 2 and Figure 3. We have compared the results using the motion planning strategy proposed in this paper, referred to as *Adaptive path*, with two other approaches. In the *Static* approach two sensor nodes are taking measurements at some static locations $(150, 300)$ and $(450, 300)$. In the *Circular path* approach the two sensors fly in circular motions around the same two locations with radius of 50 meters, and with a path period of 100 seconds. In all cases the state and parameter estimators used are identical. Obviously more thorough simulations would be required to assert that the proposed strategy is definitely better, the results from this simple example suggest that the adaptive sampling strategy leads to faster state- and parameter convergence. The resulting oil-spill concentration estimation errors and UAV paths from the strategy proposed in this paper are illustrated in Figure 4-6 for different time instants ($t \in \{0, 100, 300\}$).

V. CONCLUSIONS

In this paper we have proposed an adaptive sampling strategy for a UAV sensor network. A trajectory planner is introduced in order to improve observability of the system, and to prevent the mobile sensors to be stuck around some

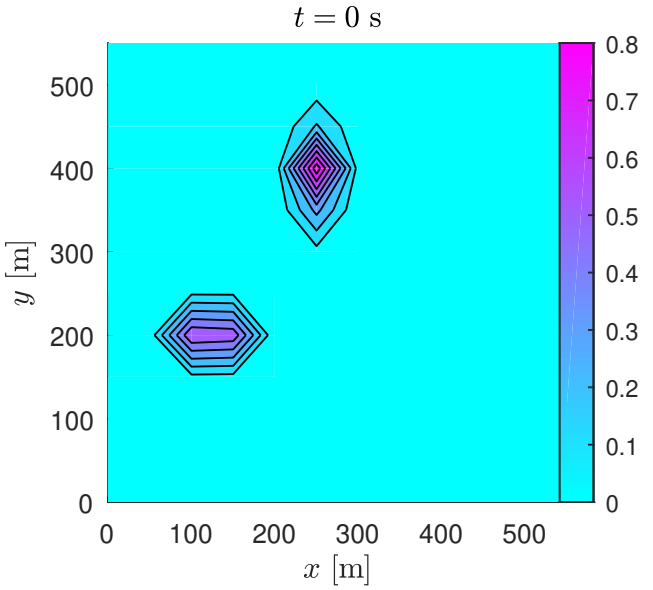

Fig. 4. Oil-spill management: Snapshot of state estimation error surface $|\chi_3(0)|$. The system has been simulated for 30 second prior to this snapshot.

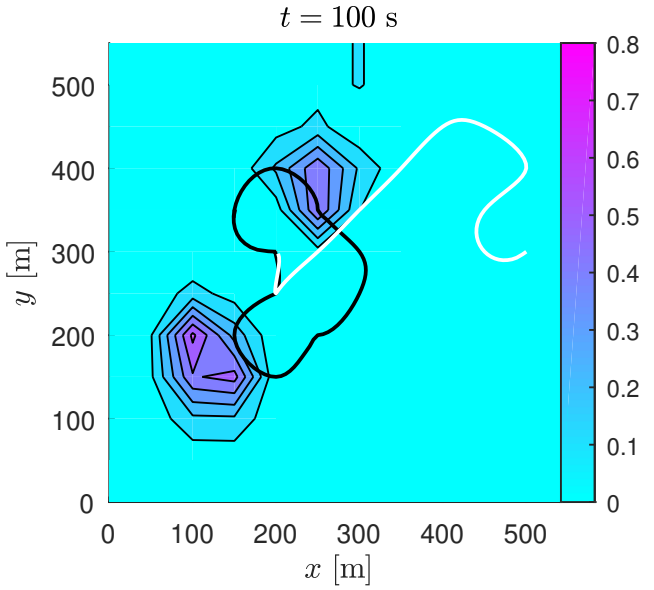

Fig. 5. Oil-spill management: Snapshot of state estimation error surface $|\chi_3(100)|$. The motions of the UAVs are illustrated with black (UAV 1) and white (UAV 2) lines.

local minima. The trajectory tracking control strategy is based on Lyapunov analysis, and we show UGAS of the closed-loop estimation, identification and trajectory tracking errors. Our approach is applied to an oil-spill example, and the benefits of the method is supported by simulations.

VI. Acknowledgements

This work was supported by the Research Council of Norway through Centers of Excellence funding scheme, Project number 223254 - Centre for Autonomous Marine Operations and Systems (NTNU-AMOS), and the INDORSE project 267793.

Appendix

To prove Theorem 1 the following propositions and lemmas will be needed:

Proposition 1: The equilibrium point $\chi_1 = \text{col}[\chi_{11}, \chi_{12}] = 0$ of $\dot{\chi}_1 = f_1(t, \chi_1)$ is UGES.

Proof: Let $V_1 := \frac{1}{2}\chi_1^\top P_1 \chi_1$, with

$$P_1 := \begin{bmatrix} K^{\text{pro}} & \Lambda M \\ M\Lambda & M \end{bmatrix} . \tag{46}$$

We see that the Lyapunov function is lower and upper bounded by $\underline{\alpha}_1(s) = \lambda_{\min}(P_1)s^2$ and $\overline{\alpha}_1(s) = \lambda_{\max}(P_1)s^2$, respectively. Furthermore, $\dot{V}_1 \leq W_1(\chi_1)$, where $W_1(\chi_1) := \chi_1 Q_1 \chi_1$ is positive definite, with

$$Q_1 := \begin{bmatrix} K^{\text{pro}} + \Lambda(D + K^{\text{der}})\Lambda & \Lambda(D + K^{\text{der}}) \\ (D + K^{\text{der}})\Lambda & D + K^{\text{der}} \end{bmatrix} . \tag{47}$$

The conclusion follows by standard arguments. ■

Lemma 1: Under Assumption 2 and 4 there exist constants c_{10}, c_{11} such that

$$c_{10} I \leq P_3(t) \leq c_{11} I \,, \tag{48}$$

for any $t \geq 0$.

The lemma is taken from [16, Lemma 1] which proof is contained in [20] and [21].

Proposition 2: Under Assumption 2, 4 and 6, the equilibrium point $\chi_3 = 0$ of (27) is Uniformly Globally Exponentially Stable (UGES).

Proof: This follows from [16, Theorem 1]. In fact, take $V_3(t, \chi_3) = \chi_3^\top P_3^{-1} \chi_3$ as a Lyapunov function candidate. We use that $\dot{P}_3^{-1}(t) = -P_3^{-1}(t)\dot{P}_3(t)P_3^{-1}(t)$, and find that $\dot{V}_3 = -\chi_3^\top (P_3(t)Q_3(t)P_3(t) + C^\top(t, \chi_{11})R_3^{-1}(t)C(t, \chi_{11}))\chi_3$. Since positive definiteness of $P_3(t)$ and its inverse follows from Lemma 1, and $Q_3(t)$ is positive definite by Assumption 6, $\dot{V}_3 \leq -c_8|\chi_3|^2/c_{10}^2$, and by standard arguments the equilibrium point of (27) is UGES. ■

Lemma 2: Under Assumption 2, 4 and 6, there exists a $c_4 > 0$ such that

$$\left|\Psi(t)\right| \leq c_4 \,, \quad \text{for any } t \geq 0 \,, \tag{49}$$

where $\Psi(t)$ is the solution to (20).

Proof: Since the system $\dot{\Psi} = A^{\text{cl}}(t, q)\Psi$ is UGES by similar argument as in Proposition 2, and the input $B(t)$ of (20) is bounded by Assumption 2, the conclusion follows. ■

Lemma 3: Under Assumptions 1, 2, 4, 5 and 6, Assumption 1 of [22] is satisfied. That is, the equilibrium point $\chi_2 = 0$ of $\dot{\chi}_2 = f_2(t, \chi_{11}, \chi_2)$ is UGAS.

Proof: $\left|\Psi(t)\right|$ is bounded by Lemma 2 and by Assumption 3, $\left|C(t, \chi_{11})\right|$ is bounded for bounded $q^{\text{ref}}(t)$ and χ_{11} which holds by Assumption 1 and Lemma 1, respectively. Therefore UGAS of the equilibrium point $\chi_2 = 0$ of $\dot{\chi}_2 = f_2(t, \chi_{11}, \chi_2)$ follows from [23, Theorem 2.16] due to persistency of excitation, Assumption 5. ■

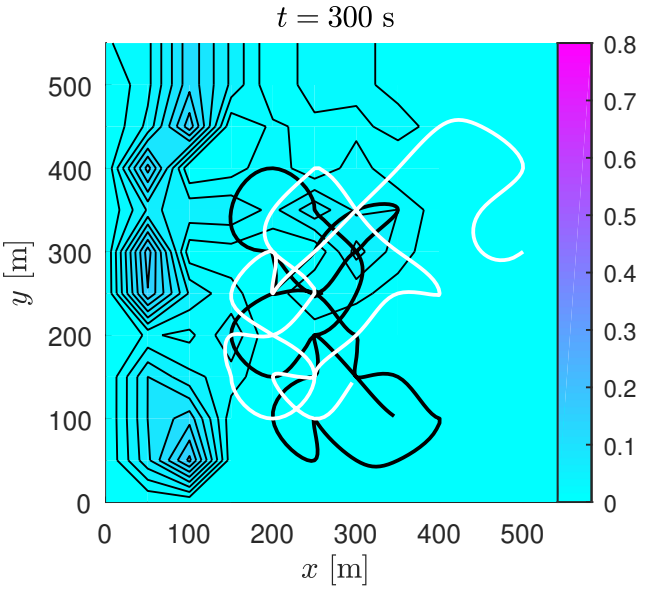

Fig. 6. Oil-spill management: Snapshot of state estimation error surface $|\chi_3(300)|$. The motions of the UAVs are illustrated with black (UAV 1) and white (UAV 2) lines.

Lemma 4: Under Assumptions 1-6, the solutions to (25)-(27) are Uniformly Globally Bounded (UGB).

Proof: Due to Propositions 1 and 2, $\chi_1(t)$ and $\chi_3(t)$ are UGB. Then, using Assumption 3 and Lemma 2 the interconnection term $g_2(t, \chi_{11})\chi_3$ in (26) is uniformly bounded. Since the equilibrium point $\chi_2 = 0$ of $\dot{\chi}_2 = f_2(t, \chi_{11}, \chi_2)$ is UGAS, due to Lemma 3, a bounded input will provide a bounded state, and the conclusion follows. ■

We are finally ready to give the proof of the main result:

Proof: [Proof of Theorem 1] Due to Proposition 1, Proposition 2 and Lemma 4, the equilibrium points of (25) and (27) are respectively UGES and UGAS, and the solutions of (25)-(27) are UGB. Finally, since $\dot{\chi}_2 = f_2(t, \chi_{11}, \chi_2)$ is UGAS by Lemma 3 the conclusion holds by [22, Lemma 2]. ■

REFERENCES

[1] C. Tricaud and Y. Chen, "Optimal mobile actuator/sensor network motion strategy for parameter estimation in a class of cyber physical systems," in *Proc. of the American Control Conference*, 2009, pp. 367–372.

[2] D. Uciński and M. Patan, "Sensor network design for estimation of spatially distributed processes," *Int. J. Appl. Math. Comput. Sci.*, vol. 20, pp. 459–481, 2010.

[3] J. A. Burns, E. M. Cliff, and C. Rautenberg, "A distributed parameter control approach to optimal filtering and smoothing with mobile sensor networks," in *Proc. of the 17th Mediterranean Conference on Control and Automation*, 2009, pp. 181–186.

[4] M. A. Demetriou and D. Uciński, "State estimation of spatially distributed processes using mobile sensing agents," in *Proc. of the American Control Conference*, 2011.

[5] Y. Chen, K. L. Moore, and Z. Song, "Diffusion boundary determination and zone control via mobile actuator-sensor networks (mas-net): challenges and opportunities," in *Proceedings of Intelligent Computing: Theory and Applications II*, 2004.

[6] J. Haugen, E. I. Grøtli, and L. Imsland, "State estimation of ice-thickness using mobile sensors," in *Proc. of the IEEE Multi-Conference on Systems and Control*, 2012, pp. 336–343.

[7] G. E. Berget, J. Eidsvik, M. O. Alver, F. Py, E. I. Grøtli, and T. A. Johansen, "Adaptive underwater robotic sampling of dispersal dynamics in the coastal ocean," in *Proc. of the International Symposium on Robotics Research*, 2019, accepted.

[8] N. K. Yilmaz, C. Evangelinos, P. F. J. Lermusiaux, and N. M. Patriklakis, "Path planning of autonomous underwater vehicles for adaptive sampling using mixed integer linear programming," *IEEE Journal of Oceanic Engineering*, vol. 33, pp. 522–537, 2008.

[9] D. Kincaid and W. Cheney, *Numerical Analysis: Mathematics of Scientific Computing*. American Mathematical Society, 2009.

[10] T. I. Fossen, *Marine Control Systems: Guidance, Navigation, and Control of Ships, Rigs and Underwater Vehicles*. Marine Cybernetics, 2002.

[11] Q. Zhang, "Adaptive observer for multiple-input-multiple-output (MIMO) linear time varying systems," *IEEE Transactions on Automatic Control*, vol. 47, pp. 525–529, 2002.

[12] ——, "Revisiting different adaptive observers through a unified formulation," in *Proc. of the IEEE Conference on Decision and Control*, 2005.

[13] R. E. Kalman, "Contributions to the theory of optimal control," *Boletin de la Sociedad Matematica Mexicana*, vol. 5, pp. 102–119, 1960.

[14] L. M. Silverman and B. D. O. Anderson, "Controllability, observability and stability of linear systems," *SIAM J. Control*, vol. 6, pp. 121–130, 1968.

[15] R. E. Kalman and R. S. Bucy, "New results in linear filtering and prediction theory," *ASME Journal of Basic Engineering*, pp. 95–108, 1961.

[16] M. S. Chen and C.-y. Kao, "Control of linear time-varying systems using forward Riccati equation," *Transactions of ASME*, vol. 119, p. 536, 1997.

[17] A. Weiss, I. Kolmanovsky, and D. S. Bernstein, "Forward-integration riccati-based output-feedback control of linear time-varying systems," in *Proc. of the 2012 American Control Conference*, 2012, pp. 6708 – 6714.

[18] D. Georges, "Energy minimization and observability maximization in multi-hop wireless sensor networks," in *Proc. of the IFAC World Congress*, 2011.

[19] K. S. Bobinyec and S. L. Campbell, "Linear differential algebraic equations and observers," in *Surveys in Differential-Algebraic Equations II*, A. Ilchmann and T. Reis, Eds. Springer, 2010, pp. 1–68.

[20] W. M. Wonham, "On a matrix riccati equation of stochastic control," *SIAM J. Control*, vol. 6, pp. 681–697, 1968.

[21] B. D. O. Anderson and J. B. Moore, "Extensions of quadratic minimization theory ii. infinite time results," *International Journal of Control*, vol. 7, pp. 473–480, 1968.

[22] E. Panteley and A. Loría, "Growth rate conditions for uniform asymptotic stability of cascaded time-varying systems," *Automatica*, vol. 37, pp. 453–460, 2001.

[23] K. S. Narendra and A. M. Annaswamy, *Stable Adaptive Systems*. Prentice-Hall, Inc., 1989, ISBN: 0-13-839994-8.